Evaluation of Corrosion Behavior of 316 L Stainless Steel Manufactured by SLM Method After Heat Treatment and Surface Treatments

S. Abdulnabi Wali[1], M. Razazi Boroujeni[2,*], S. Nosohiyan[3]

[1]Department of Materials Engineering, South Tehran Branch, Islamic Azad University,Tehran, Iran.
[2] Department of Materials Engineering, Lenjan Branch, Islamic Azad University, Isfahan, Iran.
[3] Faculty of Skills and Entrepreneurship, Isfahan Branch, Islamic Azad University, Isfahan, Iran.
Received: 08 February 2023 - Accepted: 17 May 2023

Abstract

In recent years, selective laser melting (SLM) has attracted the attention of engineering active in this field due to its controllability, the possibility of producing parts with complex shapes and good surface properties. It has been found that by performing the next operation that takes place after the production of parts by SLM method, its surface properties such as corrosion and tribological properties can be improved. In this research, two types of subsequent treatments including heat treatment and surface mechanical treatment (shot peening) were investigated on the microstructure and corrosion behavior of the 316L sample produced by SLM method. Examining the microstructure of the samples with the help of optical microscope images showed that surface treatment and heat treatment make the grains rougher and finer, respectively. The XRD pattern of the samples indicated the austenitic nature of the alloy produced by SLM method, which did not show any phase change on it by mechanical operation. While heat treatment caused the formation of oxide compounds such as chromium oxide. The corrosion behavior of the samples was evaluated using the cyclic polarization test. The results of this test showed the positive effect of the oxide layer formed during heat treatment on the corrosion behavior of the SLM sample. Also, the sample with both surface treatments showed the highest corrosion resistance due to having the lowest roughness and the presence of chromium oxide.

Keywords: Corrosion, Phasing, Heat Treatment, Selective Laser Melting.

1. Introduction

Additive manufacturing processes such as selective laser melting (SLM) are suitable for manufacturing complex industrial parts and can revolutionize the manufacturing industry. The production of austenitic stainless-steel parts by selective laser melting has been widely reported in past researches. Corrosion resistance and the possibility of recovering the passive layer in 316L parts fabricated by SLM method is a very sensitive and vital issue for their application in the industry. Although the corrosion properties of the aforementioned parts that are fabricated by SLM method and reported in the articles include discontinuous results and these reports do not overlap. Some articles refer to the excellent corrosion properties of 316L fabricated by SLM, while others report completely opposite results. This discontinuity in the reports is due to defects created during construction, such as porosity, discontinuity, and microstructural inhomogeneities. In a study [1] on 316L stainless steel produced by additive manufacturing method, immersion test in ferric chloride solution (6wt%) was performed for 48 hours.The results showed that the corrosion rate of the sample produced by the additive manufacturing method is almost five times that of the conventional sample due to the higher sensitivity of the boundaries caused by the formation of the molten pool during the manufacturing process [1]. In some research [3, 2, 1], a weak processability for 316L alloy produced by additive manufacturing method has been reported and its reason has been attributed to the presence of holes or the heterogeneity of the chemical composition (especially the separation of molybdenum element along the cell boundaries). In reviewing the results of a study that Chao et al. [4] compared the pitting corrosion behavior of 316L alloy produced by SLM method and processed 316L alloy, although the grain size and chemical composition of both alloys were almost the same. In the SLM alloy, due to the high rate of solidification, the formation of MnS was prevented and also the adjacent areas were prevented from being depleted of chromium, and as a result, it showed very good pitting corrosion resistance. In the study of Zhao et al. [5], the chemical composition and electrochemical performance of the coating film formed on the 316L alloy produced by the SLM method and also the processed alloy were investigated in the sea environment, and finally the mechanism of improving the corrosion behavior of the SLM alloy was attributed to the smaller grain size and higher grain boundary density .The operation is done after the incremental manufacturing process on the parts

*Corresponding author
Email address: mohamad.razazi@yahoo.com

to minimize the defects formed during the manufacturing process. In the case of 316L steel fabricated by SLM method, special subsequent processes have been designed to improve the properties of these parts. The surface roughness and imperfections created during construction have strongly affected the corrosion properties of these steels, and therefore, if the next operations focus on these things, they will definitely improve the corrosion [6,7]. In general, subsequent mechanical operations have also been evaluated in the studies of some researchers. For example, performing the Equal channel angular pressing (ECAP) mechanical method by Ueno et al. [8] has led to the improvement of the mechanical properties of 316L steel by changing the grains. Lu et al. [9] have investigated the dynamic plastic deformation (DPD) method, which shows that the tensile behavior of 316L steel is improved. Krawczynska et al.[10] have reported the increase of tensile and compressive properties of 316L stainless steel produced by SLM method by performing hydrostatic extrusion. In this research, by applying the energy that is applied to the surface by the mechanical method, by refining the grains and making them finer, it seems that more desirable surface properties can be achieved. During the mechanical surface treatment, in a way, it can be said that cold work is done on the SLM sample, which means an increase in the density of dislocations and residual stress, which happened simultaneously with grain modification.

In this research, the aim is to investigate the effect of different surface treatment and heat treatment separately and simultaneously on the corrosion properties of 316L steel fabricated by SLM method.

2. Materials and Methods

In this research, the selective laser melting method was used using the Tura model M120 machine and in order to make cylindrical samples with a diameter of 8 mm and a height of 12 mm made of 316L stainless steel. The device conditions were 25 W power, scanning speed of 110 mm/s, powder layer thickness of 0.05, scanning distance of 0.13 mm, substrate temperature of 100 °C. The whole process was carried out under neutral gas and argon gas. Heat treatment was performed on one of the samples, including heating the sample at a temperature of 850 degrees Celsius for 2 hours and then slowly cooling it in air. Also, on one of the samples, surface treatment was done by shot peening method with steel balls for 1 hour. On one of the samples, heat treatment and then mechanical surface treatment by shot peening method were performed. An optical microscope was used to examine the microstructure and grain sizes. Phase and structural investigations of the samples were done by X-ray diffraction test. This test was done with the APD 2000 device, the radiation angle (2θ) was 20 to 100 degrees, the time of each step was 90 seconds, and the beam used was CuKα. To evaluate the roughness of the coatings, a portable roughness meter was used and each sample was used 5 times, and finally the average value was calculated.

Finally, According to ASTM-G61 standard the cyclic polarization test was used to evaluate the corrosion resistance of the production samples in the research. At first, the samples were subjected to open circuit potential (OCP) in 3.5 wt% sodium chloride solution for a certain period of one hour to reach stable conditions. Then the cyclic polarization test was performed in the range of 250 mV below the OCP potential to 750 mV absolute with a scanning rate of 1 mV/s. To detect the upper limit of the potential (+0.75 V or +750 mV), first the potentiodynamic polarization test was performed on the SLM 316L-HT sample to determine the breakdown potential. Usually, based on the standard, 250 mV higher than the breakdown potential is selected as the upper limit, and then the reverse scan is started.

3. Results and Discussion

Fig. 1. shows the microstructure of the sample produced by the SLM method and the samples with subsequent operations. Fig. 1.a shows the microstructure of stainless steel that has austenitic grains. The point that should be mentioned is that often in the structures of 316L steel that are produced by methods such as casting, polygonal grains are seen with a higher order, while by performing the SLM process, the sample produced is less polygonal and basically does not have a specific direction.

The way of crystal arrangement of grains next to each other, in addition to flux, also depends on the two parameters of preferred crystal direction and Marangoni effect [6], and it is precisely for this reason that despite the strong thermal gradient in the laser process, all grains are not completely uniform and in the same direction. Heat treatment at the desired temperature in this research, i.e. 800 degrees Celsius, causes the recrystallization of the grains in the microstructure, which is clearly evident by the coarsening of the grains in Fig. 1.b. It should be noted that if the grain size does not grow to a large extent, it may not have much effect on the performance and pitting corrosion potential. This phenomenon is determined by two factors: (1) reducing the number of quasi-stable holes and (2) increasing the possibility of forming stable holes by modifying the grains, which may be changed by heat treatment and eventually become more or less effective [7]. Mechanical surface treatment has been able to change the shape of the grains as well as the size of the grains (Fig. 1.c).

Table. 1. The results of roughness measurement of samples.

with heat SLM +treatment mechanical treatment	with SLM mechanical treatment	with SLM heat treatment	SLM without subsequent treatment	Sample
0.22±5.061	0.77±6.451	0.42±12.888	0.85±14.490	Ra (**μ**)
0.5±6.410	0.88±7.255	0.69±16.544	18.211	Rq (**μ**)
0.97±33.552	0.34±49.055	1.1±89.489	101.520	Rz (**μ**)

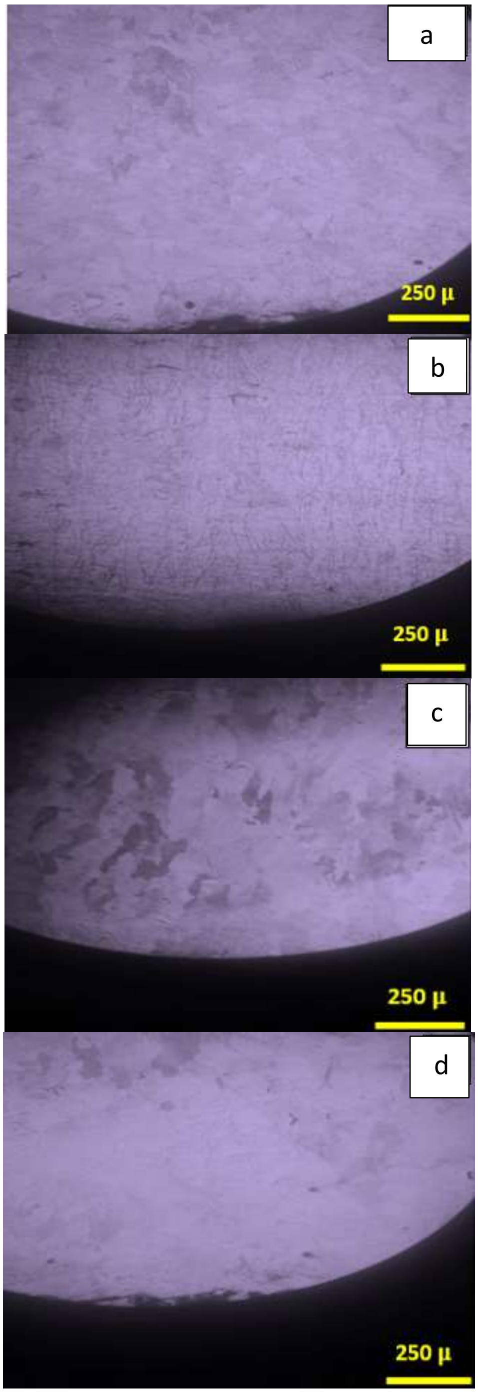

Fig. 1. Optical microscope images of the microstructure of samples produced by SLM method a) without subsequent treatment, b) with heat treatment, c) with mechanical treatment and d) with heat treatment and mechanical treatment.

However for the sample that has been subjected to mechanical surface treatment after heat treatment, this treatment has been less effective on the grains. In fact, in this case, the grains have been grown by heat treatment before the mechanical treatment of the surface, and finally, the smaller size of the grains (compared to the sample with surface treatment) has been prevented. The roughness of the coatings is reported in Table. 1. In general, the roughness of metal samples produced by SLM method is reported to be between 10 and 30 microns (the range is the roughness number Ra) [11, 12]. Moreover, the roughness of the sample after the production process in this way was 14.49 microns. The reason for the high roughness is justified due to the rapid melting and freezing process and as a result the presence of holes or inclusions in the surface of the coating. During heat treatment, due to the fact that at the temperature of heat treatment, the penetration of atoms is possible, but there is no half melting or melting of particles, practically it cannot affect the surface roughness much. While in two samples with mechanical surface treatment, the roughness has been significantly reduced. The reason for this reduction is the energetic mechanical collisions applied on the surface, which can lead to a reduction in roughness by partially melting the particles in the heights (peaks) and transferring them to the lowlands (valleys) with the aim of reducing the surface energy. In fact, it can be said that the mechanical surface treatment with a significant change in shape on the upper layers of the surface, by fragmenting the grains and plastic deformation on the surface has led to softer and smoother surfaces. The X-ray diffraction pattern of the samples can be seen in Fig. 2. In the first example, SLM (Fig. 2.a), the existing phase is only austenite with FCC crystal structure. Therefore, the alloy produced in this research has a good acceptability in terms of phase and chemical composition compared to steels produced by conventional commercial methods [13]. For all the peaks in Fig. 2.A, a broadening can be seen. According to the X-ray diffraction analysis, broadening may occur in the obtained patterns due to two phenomena: firstly, the examined piece has an amorphous phase, which is unacceptable according to the microstructural images of the samples, and the amorphousness of the product produced from 316L stainless steel material is not reported by SLM method in other studies. Secondly, the investigated material should have residual stress, which is possible for the SLM process. Therefore, the broadening of the peaks in Fig. 2.a is related to the residual stress that is created during freezing in the sample and its different layers. Heat treatment (Fig. 2.b) causes the formation of oxide phases such as iron oxide and chromium oxide, and some phase change from austenite to ferrite also occurs. In fact, due to the high amount of chromium and iron elements, preferential oxidation occurs and oxide compounds of these two elements may form on the surface. Considering that the structure of the SLM sample has dislocations and residual stress caused by the gradient and thermal stresses, heat treatment has led to the reduction of peak broadening due to the release of these dislocations and residual stress [14]. The relationship between dislocations and residual stress can be seen more fully in the X-ray diffraction pattern of the SLM sample with subsequent mechanical treatment (Fig. 2.c) so that due to the stress resulting from the mechanical process and deformation along with the change in the volume of the upper layers, the residual stress and as a result, the broadening of the peaks has increased somewhat. This is while, for sample with two subsequent operations (Fig. 2.d), the presence of oxide phases (as a result of heat treatment) and the broadening of peaks (as a result of mechanical operation) can be seen at the same time. Cyclic potentiodynamic polarization test was used to check pitting corrosion resistance of different samples. Fig. 3. shows the TOEFL potentiodynamic polarization diagram performed on the 316L-HT sample. As can be seen, the breakdown potential of this sample (starting pitting and entering the surface transition region) is around +0.442 V (+442 mV). For this reason, the reverse scan in the cyclic polarization test from the potential of +750 mV was considered for all samples. Fig. 4.a shows the cyclic polarization diagram of SLM 316L sample. As can be seen, at a certain critical current density, the stage of passivation begins. In a certain potential range, the current density remains almost constant. Then, due to the penetration of attacking anions, this layer is broken and the current density increases. Again, at the potential of +0.259 V, the secondary passive layer is formed on the bottom surface. Finally, at the potential of +0.43 V, complete breakdown has occurred and it enters the region of transition from the passive state. In the reverse scan, it can be seen that a loop is forming from the bottom of the anode branch. This loop is called hysteresis loop. Therefore, the beginning of pitting has happened in the sample. By continuing the reverse scan, it is observed that the loop cuts the cathode branch of the sample. It means that the holes created on the surface of the sample were continuously growing in such a way that they could not be filled through the corrosion products. In other words, there has been a stable growth of the hole. This indicates that if pitting occurs in the SLM 316L sample, it cannot be protected and passivated until complete destruction. The cyclic polarization diagram of SLM 316L-HT sample is also shown in Fig. 4.b. It is clearly known that at the potential of -0.154 V, the passivation stage of the sample is occurred and the current density remained almost constant until the potential of 0.513 V. The pitting potential of the sample is +0.513 V. After that, it enters the transition zone from the passive state. Again, during the reverse scanning, the loop is forming from the bottom of the anode branch, which shows that the beginning of pitting in the sample is definitely happening.

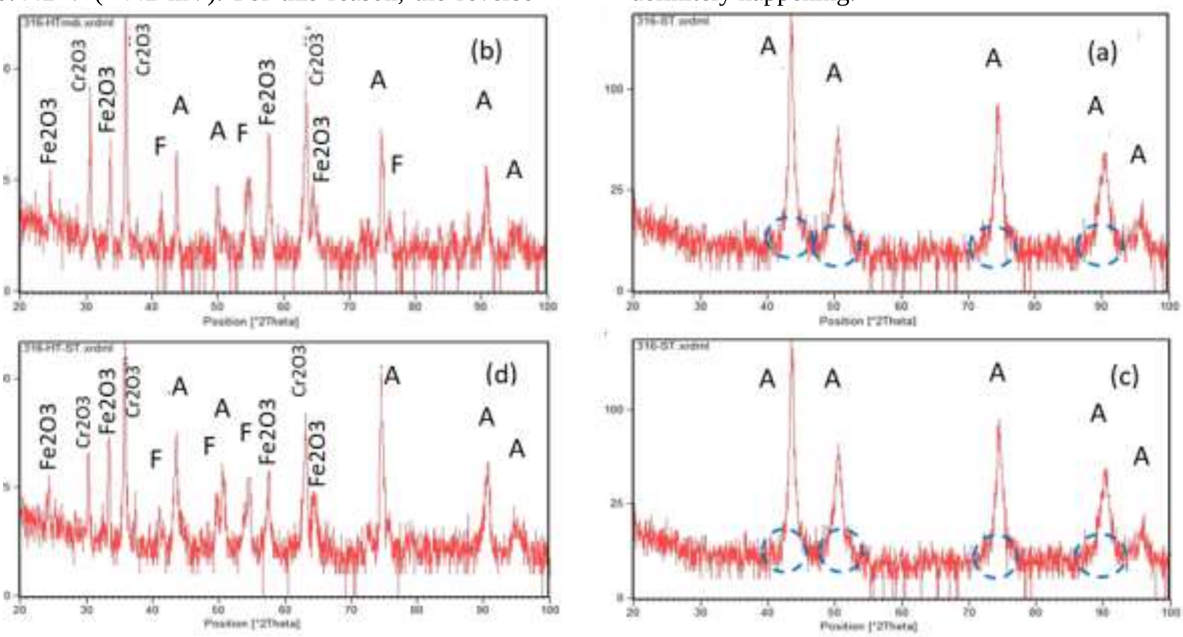

Fig. 2. XRD test results of samples produced by SLM method a) without subsequent treatment, b) with heat treatment, c) with mechanical treatment and d) with heat treatment and mechanical treatment

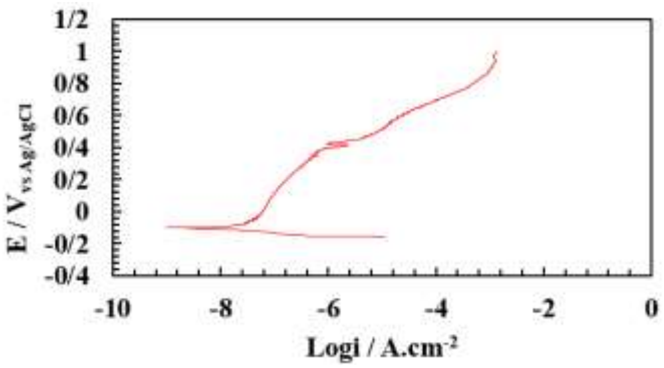

Fig. 3. Potentiodynamic polarization diagram of 316L-HT sample in the range of -0.2 to 1 V with a scanning rate of 1 mV/s to determine the breaking point and the beginning of pitting.

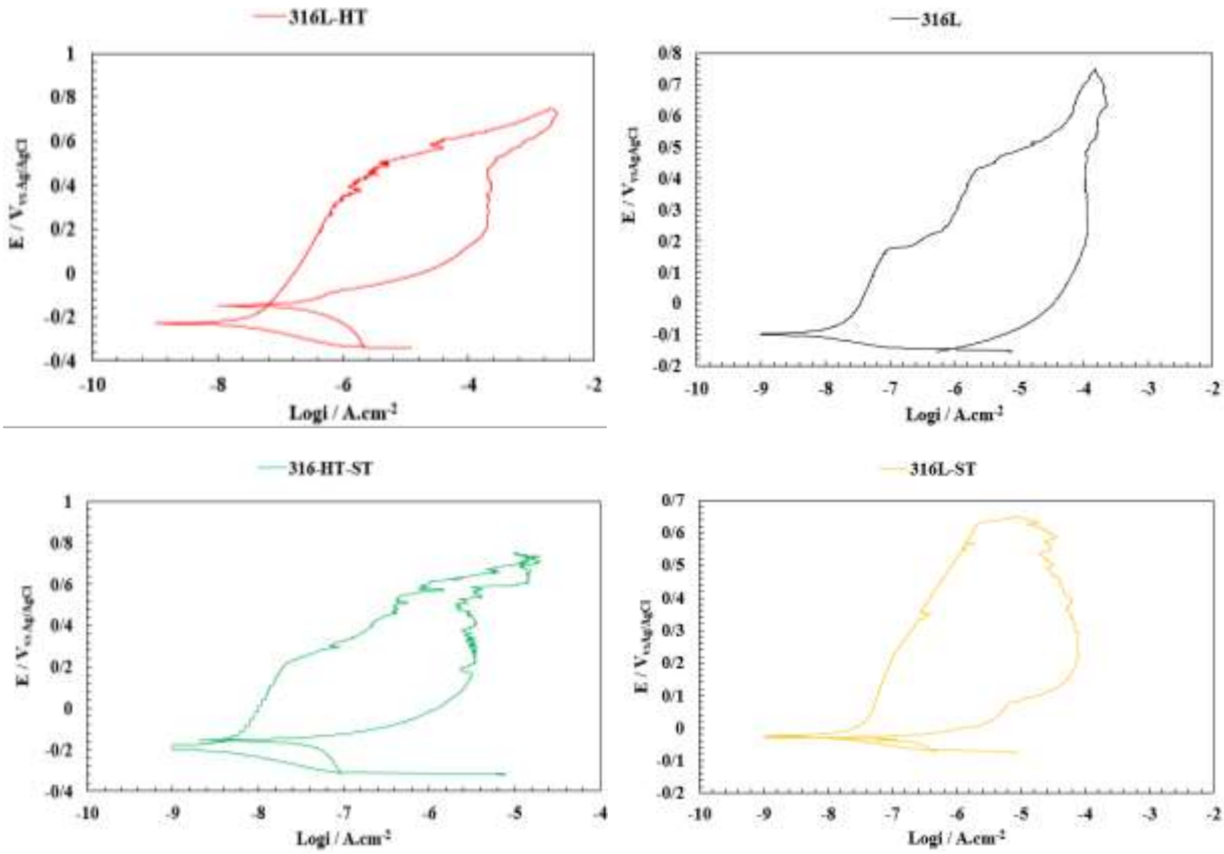

Fig. 4. Cyclic polarization diagrams of four different samples.

Table. 2. Information extracted from cyclic polarization curves.

E_{rep} (V)	ETP (V)	ip2 (A.cm^{-2})	Ep2 (V)	ip1 (A.cm^{-2})	Epp1 (V)	$I_{crit.}$ (A.cm^{-2})	$I_{cor.}$ (A.cm^{-2})	$E_{cor.}$ (V)	Sample
-	+0.43	1.3152× 10^{-6}	+0.259	6.2004 × 10^{-8}	-0.018	3.1003 × 10^{-8}	6.9984 × 10^{-8}	- 0.106	**316L**
-0.143	+0.513	-	-	6.3289 × 10^{-7}	-0.154	7.1006 × 10^{-8}	1.8001 × 10^{-8}	- 0.240	**316L-HT**
-0.156	+0.613	6.5313× 10^{-7}	+0.460	1.2960 × 10^{-8}	-0.082	8.0002 × 10^{-9}	2.9998 × 10^{-9}	- 0.156	**316L-HT-ST**
-	+0.629	-	-	2.9676 × 10^{-7}	+0.026	4.0004 × 10^{-8}	1.2001 × 10^{-8}	- 0.030	**316L-ST**

Therefore, the SLM 316L-HT sample is not resistant to pitting like the SLM 316L sample. However, it is noteworthy that, unlike the SLM 316L sample, for this sample, the reverse scan at the potential of -0.143 V cuts the anodic branch of the curve. This potential is known as protection potential or re-passivation potential. It implies that the stable growth of holes did not occur for the SLM 316L-HT sample and the holes are filled by corrosion products. In other words, due to the smaller area of the hysteresis loop of SLM 316L-HT compared to SLM 316L, the resistance to local corrosion (pitting corrosion) is much higher. The cyclic polarization diagram of SLM 316L-HT-ST sample is shown in Fig. 4.d. For this sample, the passive and protective layers are formed at two specific potentials of -0.082 and +0.460 volts. The breakdown potential for this sample is +0.613 V to enter the passive state transition region. Compared to the previous two examples, it has a more noble destruction potential. It is clear that the hysteresis loop is forming from the bottom of the anode branch, so pitting must occur. But there is no stable growth of the hole, because recrystallization happens at a potential of about -0.156 V. The hysteresis loop area of SLM 316L-HT-ST and SLM 316L-HT sample are almost equal and similar. Finally, Fig. 4.c shows the cyclic polarization diagram of SLM 316L-ST sample. By reaching a certain critical current density at the potential of +0.026 V, the ability to form the passive layer is provided. In a large potential range, the current density remains almost constant. E_b for SLM 316L-ST sample is +0.629V. After this point, entering the transition zone from the passive state occurs. If you look carefully, the hysteresis loop is formed from the bottom of the anode branch. This shows that this sample, like the three previous samples, has no resistance to pitting. Also, in the continuation of the reverse scan (decrease of the potential towards the cathode), the cathode branch of the curve is cut off. As a result, it leads to the stable growth of the hole. According to the results of Fig. 4. and Table. 2., it seems that by performing heat treatment due to the dissolution of carbides, especially chromium carbide ($Cr_{23}C_6$), it prevents the impoverishment of areas near grain boundaries from chromium. The available chromium creates a protective and strong layer of Cr_2O_3 throughout the structure, which increases the corrosion resistance of the sample, especially the resistance to pitting. It is clear that the SLM-HT-ST sample shows the lowest corrosion current density and critical current density, the lowest passivation current density and the most positive breakdown potential. Also, the re-passivation phenomenon will occur for this sample as well [15].

4. Conclusion

1. Mechanical operation makes the surface much rougher, which is possible by transferring their tension impact to the surface of the samples.
2. Performing mechanical surface treatment after thermal treatment has not been able to lead to fine grains because by performing heat treatment dislocations are released and residual stress is reduced.
3. Heat treatment has led to the growth of grains, which is due to the reduction of the density of dislocations and residual stress by accelerating the penetration process by providing the right temperature and time.
4. Heat treatment due to the creation of a layer of chromium oxide has been able to create a high protective role on the SLM sample against pitting corrosion.
5. The sample with both surface treatments showed the highest corrosion resistance due to having the lowest roughness and the presence of chromium oxide.

References

[1] C. Prieto, M. Singer, T. Cyders and D. Young, Corros., 75(2019), 140.

[2] J.R. Trelewicz, G.P. Halada, O.K. Donaldson and G. Manogharan, Jom., 68(2016), 850.

[3] D. Kong, X. Ni, C. Dong, L. Zhang, C. Man, J. Yao, K. Xiao and X. Li, Electrochim. Acta., 276(2018), 293.

[4] Q. Chao, V. Cruz, S. Thomas, N. Birbilis, P. Collins, A. Taylor, P.D. Hodgson and D. Fabijanic, Scr. Mater., 141(2017) 94.

[5] Y. Zhao, H. Xiong, X. Li, W. Qi, J. Wang, Y. Hua, T. Zhang and F. Wang, Corros. Commun. (2021).

[6] Kale, Amol B., et al., Mat. Char. 163(2020), 110204.

[7] Kong, Decheng, et al., Electrochim. Acta, 276(2018), 293.

[8] Ueno, H., et al., Acta. Mater., 59.18(2011), 7060.

[9] Lu, K., et al., Scripta. Mater., 66.11(2012), 878.

[10] Krawczynska, Agnieszka Teresa, et al., Materials & Design, 136(2017), 34-44.

[11] Wang, Di, et al., Rapid Prototyping J., (2016).

[12] Bernevig-Sava, M. A., et al., IOP Conf. Series: Mat. Sci. Eng., 572, 2019.

[13] Portella, Quentin, Mahdi Chemkhi, and Delphine Retraint, Mat. Char., 167(2020), 110463.

[14] Yin, Y. J., et al., Mat. Sci. Eng., 744(2019), 773.

[15] Chen, Hongwei, et al., Metals, 10.1(2020), 102.